PSO-Based EKF Estimator Design for PMBLDC Motor

Ahmed Hammood Abed
Electrical Engineering Department, University of Technology/Baghdad
Email: ahmadabid90@gmail.com
Dr. Mohammed Moanes E. Ali
Electrical Engineering Department, University of Technology/Baghdad
Email: dr.mohammed.moanes@uotechnology.edu.iq

Received on:21/9/2015 & Accepted on:21/4/2016

ABSTRACT

The estimation of motor state variables is an important criterion in the drive performance, especially for high accuracy required, for that reason it's-necessary to estimate rotor-position-continuously not for sixty-electrical-degrees as in most existing methods. In this work the speed and position for the rotor of Permanent Magnet Brushless DC Motor (PMBLDCM) was estimated by using extended Kalman filter (EKF), this work is divided into two parts, the first one deals with design and simulation of PMBLDCM with EKF as an estimator, the results are introduced by manually selected EKF parameters (Q & R) matrices, The second one deals with investigation the performance of the use of PSO technique to optimize the performance and operation of EKF, the main use of PSO here is to optimize value for EKF parameters (Q and R), the results proved that by tuning the EKF parameters by PSO the estimated values for speed and position is very-close-to the actual value-(estimation-accuracy is increased). The resultant error clearly decreases when tuned by EKF parameters for example at full load case the speed RMS error is 0.24 for 10μs sampling time, although the RMS error is 9 for 10μs sampling time trial and error selected EKF parameters.

Keywords: Permanent magnet Synchronous motor, Extended Kalman Filter, Particle Swarm Optimization

INTRODUCTION

A brushless DC motor is a permanent magnet synchronous motor which operates by dc current, as the name implies the brushes do not exist here, they have been replaced by electronic commutation system. In contrast to brushed motor, permanent magnet brushless dc motor (PMBLDCM) operates by means of an electronic six-step commutation system and it doesn't contain any carbon brushes. The solutions for the drawbacks of brushed DC motor and AC motors can be found in PMBLDCMs, with superior performance. PMBLDCMs have similar characteristics to the separately excited DC machines but their control is similar to the AC machines control [1]. A permanent magnet motor that has a trapezoidal-induced back emf is famous as the Permanent Magnet Brushless DC Motor (PMBLDCM). The main reason for the publicity of these machines over their counterparts is because of its control simplicity. In PMBLDCM because of the nature of the rotor and no electrical connection between the stator and rotor, it's very important to specify the direction of the magnetic field in other words it's very important to know the position of the rotor

so as to energize the concerned phases, this process is known as the commutation, there are two main ways to sense the position of the PM motors, the two methods are as follow [2]:

1) Sensored technique, by using one type of sensor, such as Hall Effect sensor, resolver, shaft encoder etc.
2) Sensorless technique, by using one type of sensorless techniques, such as, back emf detection, phase locked loop, an estimator (e.g. Extended Kalman filter)

In most existing methods, the rotor position is detected every 60 electrical degrees, which is necessary to perform current commutations. These methods are based on: 1) using the back EMF of the motor [3], [4]; 2) detection of the conducting state of freewheeling diodes in the unexcited phase [5]; and 3) the stator third harmonic voltage components [6]. Since these methods cannot provide continual rotor position estimation, they are not applicable for the sensorless drives in which high estimation accuracy of the speed and rotor position is required. In that case, it is necessary to estimate rotor position continually, not only every 60 electrical degrees. In [7], the rotor position of the PMBLDCM is estimated continually using measured motor voltages and currents with the aim of estimating flux linkage.

The aim of this research is to enhance the work of EKF by finding optimum value for its parameter using PSO technique that reduce the error between the actual and estimated position and speed, therefore makes the estimated values are closer to the real one.

The software used in this work is Matlab (8.4.0.150421) (R2014b) with m.file language. For more details about the above mentioned subject check [1], [8].

Mathematical Model of PMBLDCM

The flux distribution in PMBLDCM is trapezoidal and therefore the d–q rotor reference frame model developed for the PM synchronous motor is not applicable, given the non-sinusoidal flux distribution, it is prudent to derive a model of the PMBLDCM in phase variables. The derivation of this model is based on the assumptions that the induced currents in the rotor due to stator harmonic field are neglected and iron and stray losses are also neglected. Damper windings are not usually a part of the PMBLDCM and damping is provided by the inverter control. The motor is considered to have three phases even though for any number of phases the derivation procedure is valid [8].

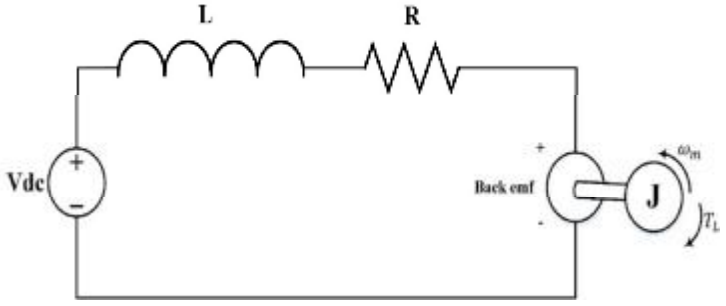

Figure (1) per phase equivalent circuit of PMBLDC motor

The equation of torque:

$$T_e = J\frac{d\omega}{dt} + B\omega + T_L \quad \text{..... (1)}$$

And electrical rotor speed and position are related by:

$\frac{d\theta_r}{dt} = \frac{P}{2}\omega_m$ …….. (2)

The instantaneous induced emfs can be written as:

$e_{ats} = f_{as}(\theta_r)\lambda_p\omega_m$ …….. (3)

$e_{bts} = f_{bs}(\theta_r)\lambda_p\omega_m$ …….. (4)

$e_{cts} = f_{cs}(\theta_r)\lambda_p\omega_m$ …….. (5)

Where function$f_{as}(\theta_r)$,$f_{bs}(\theta_r)$, $f_{cs}(\theta_r)$ has the same form as e_{as},e_{bs} and e_{cs} with a most magnitude of ± 1. The induced emfs do not have sharp corners as shown in trapezoidal functions but have rounded edges. It is because the emfs are the derivatives of the flux linkages and the flux linkages are continuous functions and fringing also makes the flux density functions smooth with no sudden edges [8], [9].

The electromagnetics torque can be written as:

$T_e = \lambda_p[f_{as}(\theta_r)i_a + f_{bs}(\theta_r)i_b + f_{cs}(\theta_r)i_c]$ (N.m) …….. (6)

The state space equation of the PMBLDCM is as follow:

$\dot{x} = Ax + Bu$ …….. (7)

$y = Cx$ …….. (8)

Where:

$x = [i_a \quad i_b \quad i_c \quad \omega_m \quad \theta_r]$ …….. (9)

$$A = \begin{bmatrix} -R_s/L_1 & 0 & 0 & -(\lambda_p/J)\,f_{as}(\theta_r) & 0 \\ 0 & -R_s/L_1 & 0 & -(\lambda_p/J)\,f_{bs}(\theta_r) & 0 \\ 0 & 0 & -R_s/L_1 & -(\lambda_p/J)\,f_{cs}(\theta_r) & 0 \\ -(\lambda_p/J)\,f_{as}(\theta_r) & -(\lambda_p/J)\,f_{bs}(\theta_r) & -(\lambda_p/J)\,f_{cs}(\theta_r) & -B/J & 0 \\ 0 & 0 & 0 & P/2 & 0 \end{bmatrix} \ldots (10)$$

$$B = \begin{bmatrix} -1/L_1 & 0 & 0 & 0 \\ 0 & -1/L_1 & 0 & 0 \\ 0 & 0 & -1/L_1 & 0 \\ 0 & 0 & 0 & -1/J \\ 0 & 0 & 0 & 0 \end{bmatrix} \ldots\ldots (11)$$

Where: $L_1 = L - M$

$u = [v_{as} \quad v_{bs} \quad v_{cs} \quad T_L]^t$ …….. (12)

Description of the Estimation Algorithm

Extended Kalman filter is an observer based on Taylor series which can handle almost every nonlinear system. Time domain model of PMBLDCM is shown in Fig. (2).

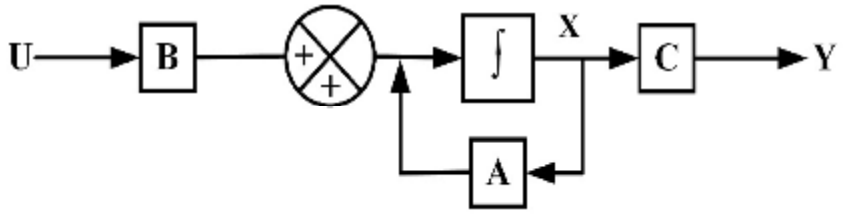

Figure (2) state space model

The timed discreet state spaced models of a PMBLDCM must are gained. If the continual state spaced models are sampled within sampling timed intervals T_s, which are selection, and should are make to subtend both the totals calculation times of a filter also grant a rational integral precision, which is fully ten times lower than the motor timed constants ($T_s = L_s/R_s$), then a matrices which the discrete-time system could be gained by Euler's approach [9], [11].

The extended Kalman filter consists of essentially two mains steps, the prediction step and the correction (filtering) step. Through a prediction step, next predicted values of a state $X(k+1)$ and a predicted state covariance matrix (P) are acquired. For that aim, a state variable equation for a PMBLDCM is applied, at a framework covariance matrix (Q). During the filtering step, the filter states ($\hat{X}$) is acquired from the predicted estimates through combing a correction expression to a predicted value (X), this correction expression is [12]:

$K_e = K(Y - \hat{Y})$…….……...……..... (13)

Where: $e = (Y - \hat{Y})$ a fault expression. Such error is reduced in the EKF. The framework of the Extended Kalman Filter (EKF) is shown in Figure (3) and Figure (4) describes the connection between EKF and PMBLDCM minutely.

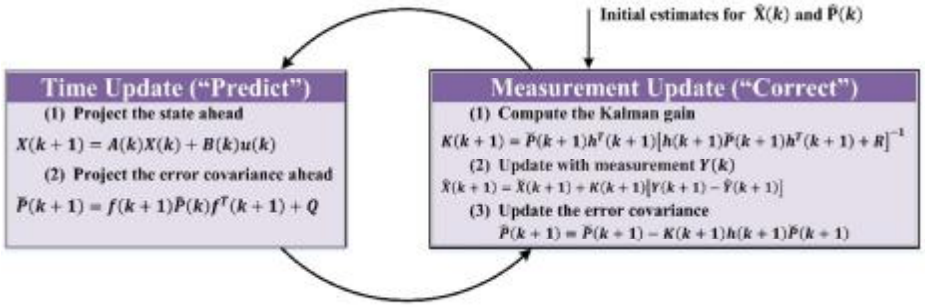

Figure (3) operation of EKF

θ_r, rotor position, are required in order to have functions $f_{as}(\theta_r)$,$f_{bs}(\theta_r)$ and $f_{cs}(\theta_r)$, the state estimates are obtained in the following stages:

Stage 1: Initialize of a state vector parameters ($X_\circ, Q_\circ, R_\circ, and\ P_\circ$).

Stage 2: Prediction of ($X(k+1)$).

$X(k+1) = A(k)X(k) + B(k)u(k)$……..... (14)

Stage 3: Covariance estimation ($\check{P}(k+1)$).

$\check{P}(k+1) = f(k+1)\hat{P}(k)f^T(k+1) + Q$……...……..... (15)

$f(k+1) = {}^{\partial}/_{\partial x}[AX + BU]_{x=\hat{x}(k+1)}$……..... (16)

Stage 4: Determine the gain.

$K(k+1) = \check{P}(k+1)h^T(k+1)\left[h(k+1)\check{P}(k+1)h^T(k+1) + R\right]^{-1}$…..... (17)

$h(k+1) = {}^{\partial}/_{\partial x}[CX]_{x=\hat{x}(k+1)}$……...……..... (18)

Stage 5: Determine ($\hat{X}(k+1)$)

$\hat{X}(k+1) = \check{X}(k+1) + K(k+1)\left[Y(k+1) - \hat{Y}(k+1)\right]$……..... (19)

$\hat{Y}(k+1) = C\check{X}(k+1)$……..... (20)

Stage 6: Finding the error covariance matrix

$\hat{P}(k+1) = \check{P}(k+1) - K(k+1)h(k+1)\check{P}(k+1)$..... (21)

For more details about the above mentioned subject check [12], [13], and [14].

Simulation of the Proposed Estimator

In this work, EKF is designed and implemented for the estimation of speed and rotor position of PMBLDCM, and the motor could run at low speed with acceptable accuracy. The dynamic model necessary to study both the steady state and transients of the motor drive system characteristic .

The resolver gives pure rotor position and it was reformed to rotor speed by using the integrating device. The rotor a speed was compared to its reference signal and the difference (error) is amplified by using the speed controller [8] . The gain of the speed controller provides the reference torque T_e^*. In the balance of three phase system, only two phases are conducted each time, and are being in series, the rotor position hanger-on equations are similar in signs of the motor phase currents, due to this relationships in signs, the simplification of the torque expression will lead to derive the current command as:

$$T_e^* = 2I_p^* \lambda_p \quad (22)$$

$$I_p^* = \frac{T_e^*}{2\lambda_p} \quad (23)$$

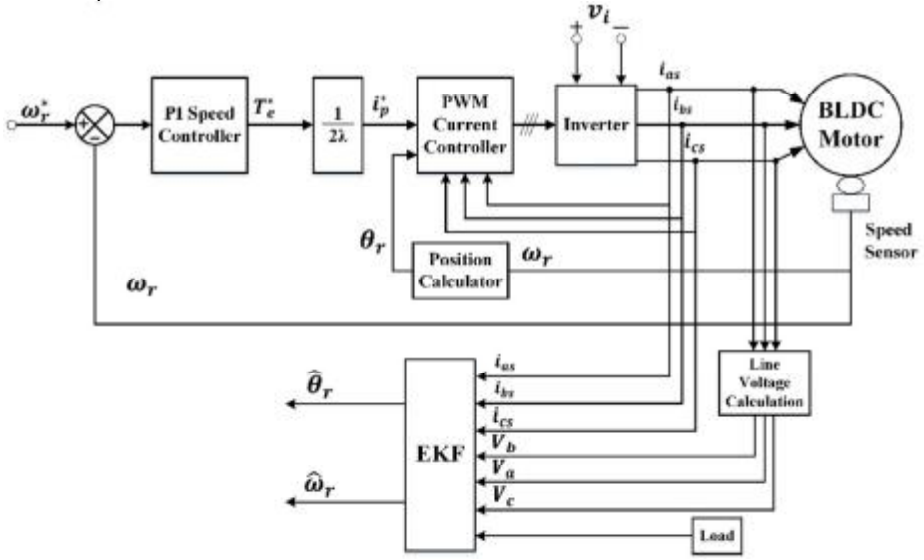

Figure (4) PMBLDCM-EKF drive scheme

The singular stator phase current orders are produced from the current magnitude order and outright rotor position . These current orders are compared to the particular feedback stator current and the resulting errors are amplified using PWM, the results are the switching signals that are supplied to the inverter switches. The model is expressed with the following assumptions [12].

- Deviation of the motor speed is negligible $\frac{d\omega}{dt} = 0$;
- Motor inductance is assumed to be constant;
- The effect of the saturation on the magnetic circuit of the motor is considered to be negligible.

[9] Represents the flow chart of PSO.

Simulation Results

The ratings of PMBLDCM used in this work are: 1 hp, 4000 rpm, 4-poles (2 pole-pairs). The simulation results are divided into two parts, first part includes the results without using PSO technique (randomly selected values of Q and R) and it could be noticed that the actual and estimated (speed and position), the second part will include the results of the proposed work.

Simulations results of a step speed reference input is 0-418.88 rad/sec for the PWM current controllers. The rotor is at standstill at time zero . With the beginning of speed reference , the speed difference (error) and torque reference reach an ultimate amount, which is restricted to twice of the rated torque in this event. The current is formed to go after the reference by the current controller . Because of that, the electromagnetic torque goes after its reference more closely. The torque ripples are because of the current ripples created by the switching . The PWM control treated in this study is operating at 5 kHz and the current controller has an amplification amount of 120 for current difference (errors) that are used with PWM to produce the switching logic signals of the inverter switches .

The PI controller parameters for the drive model are as follow:

$K_p = 0.984, K_i = 6.695$

In proposed work, the PSO algorithm here creates random values for Q and R, the system will be tested with these values then choose the optimum value is chosen that gives the minimum root mean square error between the real and evaluated signals. The constraint here is the Root Mean Squared (RMS) of the error between the actual and evaluated values . These steps are summarized in algorithm (25) Equation (24) shows the RMS equation used in this work [15] [16].

$$RMS = \frac{\sqrt[2]{e_1^2 + e_2^2 + e_3^2 + e_3^2 + e_4^2 + \cdots\cdots\cdots + e_n^2}}{n} \quad \ldots\ldots\ldots\ldots\ldots\ldots (24)$$

Where:

e: The error between the actual and estimated value at each sampling time

n: Number of the total samples- (The number of times for program execution).

Normalizing the RMS ease the comparison between scales

$$NRMS = \frac{RMS}{y_{max} - y_{min}} \quad \ldots\ldots\ldots\ldots\ldots\ldots\ldots\ldots\ldots\ldots\ldots\ldots\ldots\ldots\ldots\ldots\ldots\ldots (25)$$

Where:

y_{max}:Maximum value in the scale

y_{min}: Minimum value in the scale

Actual and Estimated Results for EKF Parameters (Q and R)

The response of EKF with PMBLDCM tuned by trial and error method for different cases; in this section is divided into two parts, the first one is with sampling time of $100\mu s$, and the second one is with 10 μs each part has been subdivided into three cases (no load, full load and over load), of course for last three cases the load is submitted after the motor speed reaches its steady state as shown below [16]:

Case study-1: no load ($T_{Load} = 0$)

In this case it is noticed that the actual and estimated speeds grow up until they meet after 43ms, see Figure (5-a) and (5-b).

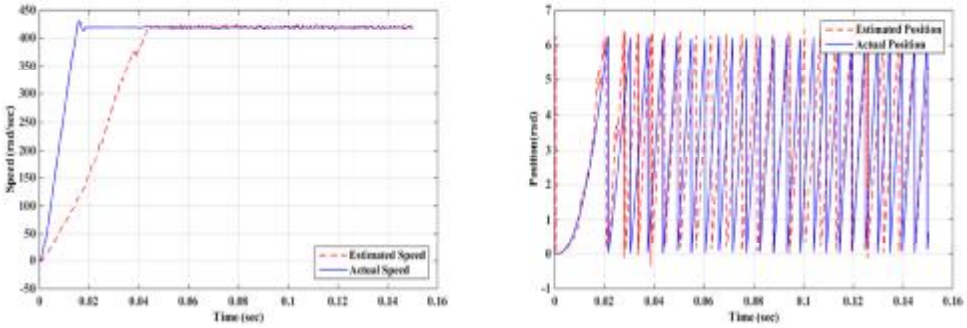

(a) (b)

Figures (5) Shows results of classical method (no-load case study and sampling time (100μs)) a) Actual and estimated speeds, b) Actual and estimated position

Case study-2: full load ($T_{Load} = full\ load$)

In this case it is noticed that the actual and estimated speeds are grow up until they meet after t=44ms, the load is introduced at time=50 ms and removed at t=100ms, see Figure (6-a) and (6-b).

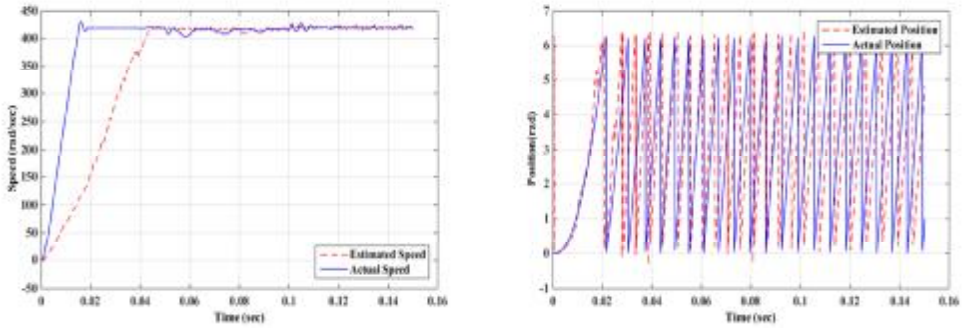

(a) (b)

Figures (6) Results of classical method (full-load case study and sampling time (100μs)) a) Actual and estimated speeds, b) Actual and estimated positions

Case study-3: Over load ($T_{Load} = 1.2 \times full\ load$)

In this case it is noticed that the actual and estimated speeds grow up until they meet after t=44ms, the load is introduced at time=50 ms and removed at t=100ms, see Figure (7-a) and (7-b).

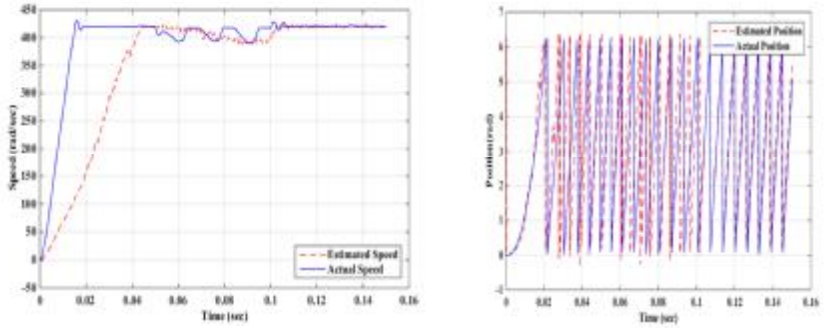

(a) (b)

Figures (7) Results of classical method (over load case study and sampling time (100μs)) a) Actual and estimated speeds, b) Actual and estimated positions

- **Now the following results are of sampling time 10μs**
-

Case study-1: no load (T_{Load} = 0)

In this case it is noticed that the actual and estimated speeds grow up until they meet after t=41.7ms, the drive here operates at no load as shown in Figure (8-a) and Figure (8-b).

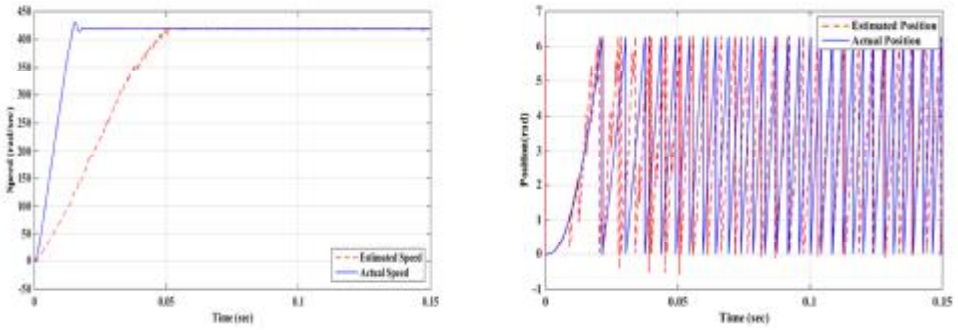

(a) **(b)**

Figure (8) Results of classical method (no-load case study and sampling time (10μs)) a) Actual and estimated speeds, b) Actual and estimated positions

Case study-2: full load ($T_{Load} = full\ load$)

In this case it is noticed that the actual and estimated speeds grow up until they meet after t=41.7ms, the load is introduced at time=50 ms and removed at t=100ms, see Figure (9-a) and (9-b).

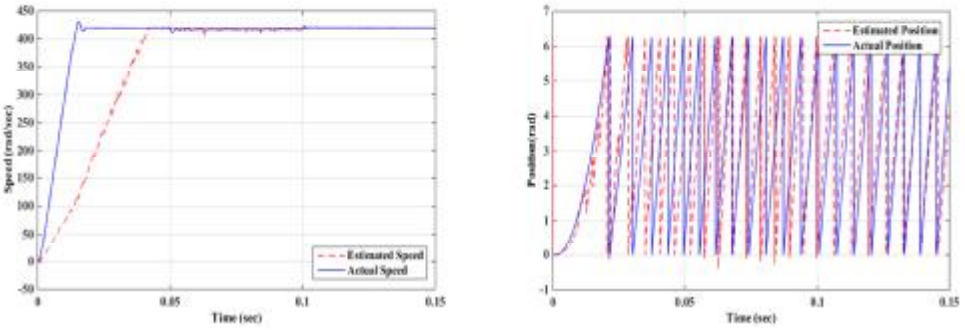

(a) (b)

Figure (9) Results of classical method (full-load case study and sampling time (10μs)) a) Actual and estimated speeds, b) Actual and estimated positions

Case study-3: Over load ($T_{Load} = 1.2 \times full\ load$)

In this case it is noticed that the actual and estimated speeds grow up until they meet after t=41.7ms, the load is introduced at time=50 ms and removed at t=100 ms, see Figure (10-a) and (10-b).

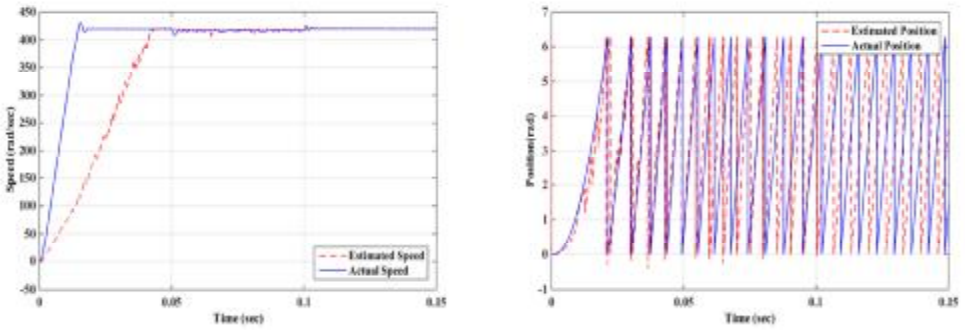

(a) (b)

Figure (10) Results of classical method (over load case study and sampling time (10μs)) a) Actual and estimated speeds, b) Actual and estimated positions

Table (1) Root mean square error results of the classical method

		The error for the results of the classical method					
		Percentage Error			Percentage Error		
		Sampling Time: 10 µs			Sampling Time: 100 µs		
		Speed	Position	Running Time (Sec.)	Speed	Position	Running Time (Sec.)
Load	No Load	6.22	1.54	2.635	10.74	3.57	1.02
	Full load	9	3.9	2.812	13.24	4.8	1.5
	Over Load	10.37	4.2	2.948	14.82	6.1	1.7

Results for the Proposed Method to Select EKF Parameters (Q and R)

In this section, tuning of EKF parameters is performed by using PSO technique according to minimum root mean square value for the difference between the actual and estimated speeds and positions. The same procedure is repeated with 100μs sampling time, the case of the load that is submitted to the motor to test the stability of the estimator at low and heavy loads shows its performance, ability and continuity. Time taken by PSO algorithm to find the values of Q and R depend on sampling time, for 100μs the time is 45 minute [16], this results are compared with other researches [4], [5], [6], PSO here select the optimum values for Q and R, which give less RMS error.

Case study-1: no load ($T_{Load} = 0$)

In this case it is noticed that the actual and estimated speeds grow up together, the drive here operates at no load, see Figure (11-a) and (11-b).

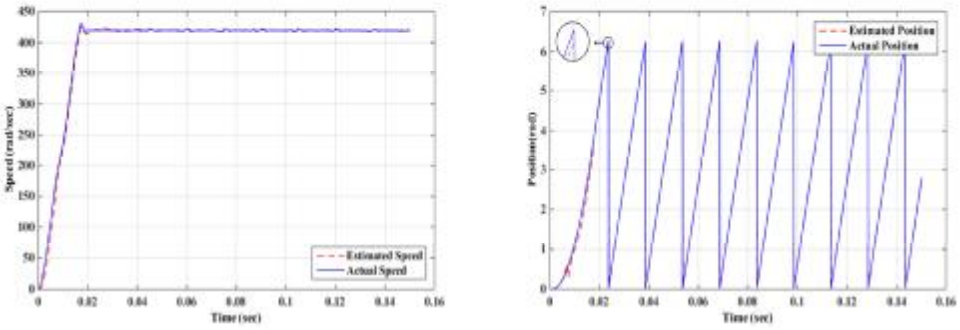

(a) (b)

Figures (11) Results of the proposed work (no-load case study and sampling time (100µs)) a) Actual and estimated speeds, b) Actual and estimated positions

Case study-2: full load ($T_{Load} = full\ load$)

In this case it is noticed that the actual and estimated speeds grow up together, the load is introduced at time=50 ms and removed at t=100ms, see Figure (12-a) and (12-b).

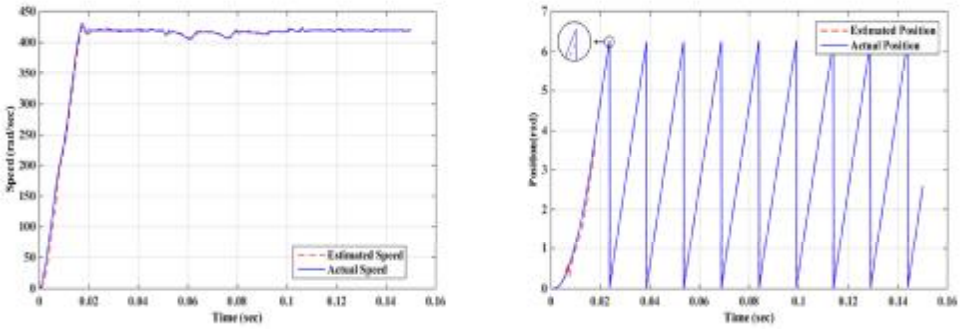

(a) (b)

Figures (12) Results of the proposed work (full-load case study and sampling time (100μs)) a) Actual and estimated speeds, b) Actual and estimated positions

Case study-3: Over load ($T_{Load} = 1.2 \times full\ load$)

In this case it is noticed that the actual and estimated speeds grow up together, the load is introduced at time=50 ms and removed at t=100ms, see Figure (13-a) and (13-b).

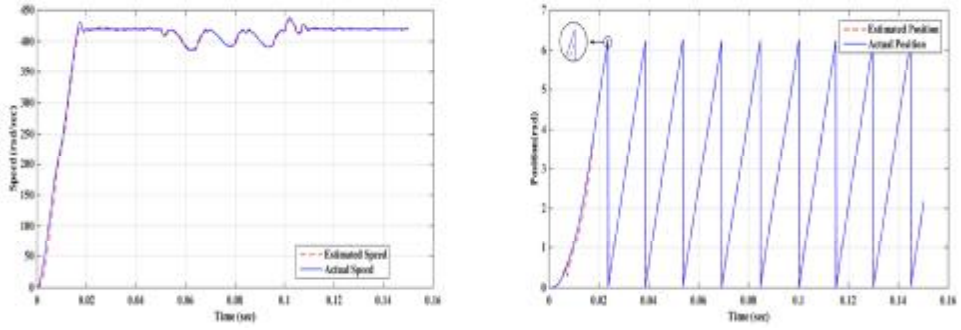

(a) (b)

Figures (13) Results of the proposed work (over-load case study and sampling time (100μs)) a) Actual and estimated speeds, b) Actual and estimated positions

- **Now the following results are for sampling time 10μs**

Case study-1: no load ($T_{Load} = 0$)

In this case it is noticed that the actual and estimated speeds grow up together, the drive here operates at no load, see Figure (14-a) and (14-b).

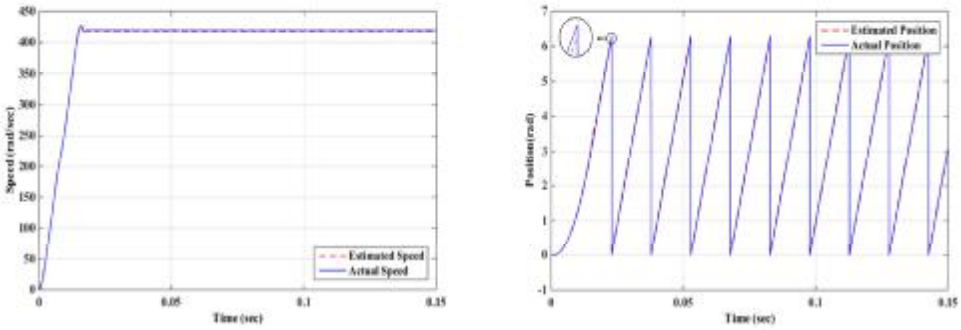

(a) (b)

Figure (14) Results of the proposed work (no-load case study and sampling time (10μs)) a) Actual and estimated speeds, b) Actual and estimated positions

Case study-2: full load ($T_{Load} = full\ load$)

In this case it is noticed that the actual and estimated speeds grow up together, the load is introduced at time=50 ms and removed at t=100ms, see Figure (15-a) and (15-b).

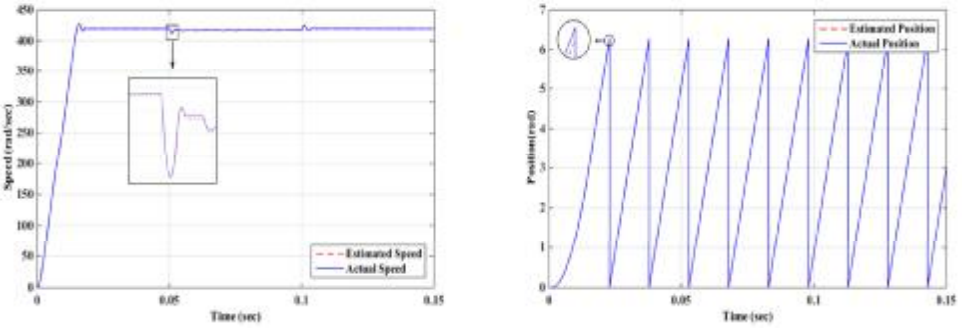

(a) (b)

Figure (15) Results of the proposed work (full-load case study and sampling time (10μs)) a) Actual and estimated speeds, b) Actual and estimated positions

Case study-3: Over load ($T_{Load} = 1.2 \times full\ load$)

In this case it is noticed that the actual and estimated speeds grow up together, the load is introduced at time=50 ms and removed at t=100ms, see Figure (16-a) and (16-b).

In this case it is noticed that the actual and estimated speeds grow up together, the load is introduced at time=50 ms and removed at t=100ms, see Figure (16-a) and

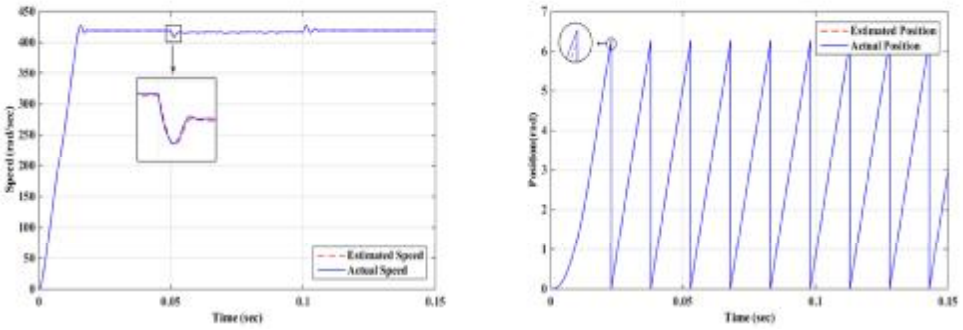

(a) (b)

Figure (16) Results of the proposed work (over load case study and sampling time (10μs)) a) Actual and estimated speeds, b) Actual and estimated positions

Table (2) Root mean square error results of the proposed work

		The error for the results of the proposed work					
		Percentage Error			**Percentage Error**		
		Sampling Time: 10 μs			**Sampling Time: 100 μs**		
		Speed	**Position**	**Running Time (Sec.)**	**Speed**	**Position**	**Running Time (Sec.)**
Load	**No Load**	**0.2**	**0.01**	**2.235**	**0.6**	**0.1**	**0.985**
	Full load	**0.24**	**0.09**	**3.233**	**0.75**	**0.19**	**1.278**
	Over Load	**0.37**	**0.16**	**3.572**	**0.78**	**0.28**	**1.499**

CONCLUSIONS

From the previous results the following points can be discussed:

The results introduced in the proposed work are much better than those of classical method as seen from Tables (1) and (2), it is obvious from these tables that the results are improved very clearly, the reason is in the nature of PSO technique which specifies the optimum parameters based on the minimum error between the actual and estimated values. These results show the superiority of the estimator based on PSO versus the trial and error method.

The drive was tested in different cases of load, and the estimator behavior is very good, when load is applied after a specified time, the results showed that the estimator is not affected.

It is clearly showed that as the sampling time decrease, the results will be more accurate but with more running time and vice versa for example, in Table (2) at

($10\mu s$) sampling time, in the no load case study the RMS error of speed is 0.2% and running time (2.235sec.) and at ($100\mu s$) sampling time for the same table the running time is (0.985sec.) the RMS error of speed is 0.1%.

The parameters values of PMBLDC motor used in the simulation are as below:

Table (3) the parameters values of PMBLDC motor

Rated Power (P_{out})	746	W
Rated voltage V(L-L)	160	V
Rated Speed (N)	4000	$r.p.m$
Rated Current (I)	8.5	Amp
Rated Torque (T)	1.7809	$N.m$
Number of pole pairs(P)	4	Poles
Stator resistance (R_s)	0.7	Ohm
Stator inductance ($L_s - M$)	5.21	mH
Viscous Friction (B)	0	$N.m/rad/sec$
Moment of Inertia (J)	2.2e-4	$Kg.m^2$

REFERENCES:

[1] Xia, Chang-Liang, "Permanent Magnet Brushless DC Motor Drives and Controls", John Wiley & Sons, Singapore, 2012

[2] José Carlos Gamazo-Real, Ernesto Vázquez-Sánchez, Jaime Gómez-Gil, "Position and Speed Control of Brushless DC Motors Using Sensorless Techniques and Application Trends", Volume: 10, Issue: 7, Pages: 6901-6947, ISSN 1424-8220, Spain, 2010

[3] K. Iizuka, H. Uzuhashi, M. Kano, T. Endo, and K. Mohri, "Microcomputer control for sensorless brushless motor," IEEE Trans. Ind. Applicat., vol. IA-21, pp. 595–601, May/June 2005.

[4] R. C. Beccerra, T. M. Jahns, and M. Ehsani, "Four quadrant sensorless brushless motor," in Proc. IEEE APEC'91, 2005, pp. 202–209.

[5] S. Ogasawara and H. Akagi, "An approach to position sensorless drive for brushless dc motors," in Conf. Rec. IEEE-IAS Annu. Meeting, 2007, pp. 443–447.

[6] J. C. Moriera, "Indirect sensing for rotor flux position of permanent magnet AC motors operating in wide speed range," in Conf. Rec. IEEE-IAS Annu. Meeting, 2008, pp. 401–407.

[7] N. Ertugrul and P. P. Acarnley, "A new algorithm for sensorless operation of permanent magnet motors," IEEE Trans. Ind. Applicat., vol. 30, pp. 126–133, Jan./Feb. 2010.

[8] R. Krishnan, "Permanent Magnet Synchronous and Brushless DC Motor Drives", CRC Press, USA, 2010

[9] D. Lenine, B. Rami Reddy, S. Vijay Kumar, "Estimation of Speed and Rotor Position of BLDC Motor using Extended Kalman Filter", ICTES, pp.433-440, Tamil Nadu. India, Dec. 20-22, 2007.

[10] Alex Simpkins, Emanuel Todorov, "Position Estimation and Control of Compact BLDC Motors Based on Analog Linear Hall Effect Sensors", American Control Conference Marriott Waterfront, Baltimore, MD, USA June 30-July 02, 2012

[11] Ejlali, A, Soleimani, J., "Sensorless Vector Control of 3-phase BLDC Motor Using a Novel Extended Kalman", Electr. Eng. Dept., Iran Univ. of Sci. & Technol.

(IUST) , Tehran, Iran, IEEE, Advances in Power Conversion and Energy Technologies, 2012
[12] Peter Vas, "Sensorless Vector and Direct Torque Control", Oxford University Press, 1998, England.
[13] Grewal and Andrews, "Kalman Filtering Theory and Practice Using MATLAB", Wiley-IEEE Press, 2001
[14] Vedran Kordić, "Kalman Filter", Vienna University of Technology Austria, European Union, Intech puplisher, 2002
[15] Choukroun, D., Oshman, Y., Thienel, J., "Advances in Estimation, Navigation, and Spacecraft Control", Springer; 2015 edition Jan- 3-2015, USA.
[16] Ahmed H. Abed, "PSO-Based EKF Estimator Design for PMBLDC Motor", M.Sc. Thesis, University of Technology, 2015